



SUBJECT AREAS:

METAL-ORGANIC
FRAMEWORKS

CRYSTAL ENGINEERING

ORGANIC-INORGANIC
NANOSTRUCTURES

POROUS MATERIALS

A Rationally Designed Nitrogen-Rich Metal-Organic Framework and Its Exceptionally High CO₂ and H₂ Uptake Capability

Xiao-Jun Wang^{1*}, Pei-Zhou Li^{1*}, Yifei Chen², Quan Zhang¹, Huacheng Zhang¹, Xiu Xiang Chan¹, Rakesh Ganguly¹, Yongxin Li¹, Jianwen Jiang² & Yanli Zhao^{1,3}

Received
22 October 2012

Accepted
4 January 2013

Published
28 January 2013

Correspondence and
requests for materials
should be addressed to
J.J. (chejj@nus.edu.sg)
or Y.Z. (zhaoyanli@
ntu.edu.sg)

* These authors
contributed equally to
this work.

¹Division of Chemistry and Biological Chemistry, School of Physical and Mathematical Sciences, Nanyang Technological University, 21 Nanyang Link, 637371, Singapore, ²Department of Chemical and Biomolecular Engineering, National University of Singapore, 117576, Singapore, ³School of Materials Science and Engineering, Nanyang Technological University, 639798, Singapore.

On the way towards a sustainable low-carbon future, the design and construction of chemical or physical adsorbents for CO₂ capture and clean energy storage are vital technology. The incorporation of accessible nitrogen-donor sites into the pore walls of porous adsorbents can dramatically affect the CO₂ uptake capacity and selectivity on account of the dipole-quadrupole interactions between the polarizable CO₂ molecule and the accessible nitrogen site. In the present work, a nitrogen-rich *rth*-type metal-organic framework (MOF) was constructed based on rational design and careful synthesis. The MOF presents exceptionally high uptake capacity not only for CO₂ but also for H₂, which is attributed to favorable interactions between the gas molecules and the nitrogen-rich triazole units of the MOF proved by both experimental measurements and theoretical molecular simulations.

Owing to their permanent porosity, high surface area, large pore volume, and adjustable pore size and shape, metal-organic frameworks (MOFs) have been extensively investigated in the past decades and have shown highly promising applications in gas storage, molecular recognition and separation, heterogeneous catalysis, and biomedical area^{1–7}. Typically, MOFs are built by the self-assembly of metal ions or clusters and polytopic bridging ligands under solvothermal conditions^{6,7}. In contrast to inorganic porous materials such as zeolites or activated porous carbons, numerous choices of organic linkers together with many coordination geometries indicate that MOFs could be tailored by judicious combinations of the building blocks for specific applications^{6–9}. Theoretically, the incorporation of accessible nitrogen-donor groups, such as pyridine, imidazole, and tetrazole, into the pore walls of porous materials can dramatically affect the gas uptake capacity and selectivity of the materials, especially for CO₂ capture on account of the dipole-quadrupole interactions between the polarizable CO₂ molecule and the accessible nitrogen site¹⁰. Literature reports also indicated that the incorporation of accessible nitrogen-donor groups into the porous materials could enhance the CO₂ uptake capacity and selectivity^{11–16}. Such approach is strategically important for developing a low-carbon future by increasing the capacity of selective CO₂ capture and by enhancing the storage capacity of clean energy source, such as H₂^{1,9,11–18}. However, competitive coordination of these Lewis basic nitrogen sites with metal ions or clusters is a great challenge in direct synthesis of MOFs^{19,20}.

Recently, rational design and synthesis of MOFs with target superstructures and desired physical properties have been significantly facilitated by the conceptual approach of reticular chemistry^{21,22}, where *in-situ* generated metal-cluster secondary building units (SBUs) are connected by decorated organic linkers in a predetermined ordered network, as exemplified in a series of isoreticular IRMOF-*n* materials derived from prototypical MOF-5 superstructure. As an extension of the SBU approach, metal-organic polyhedra (MOPs) with large size as well as high symmetry and connectivity have recently been employed as supermolecular building blocks (SBBs) for the constructions of novel MOFs^{23–25}. This strategy offers an improved control over the topology in the preparation of MOFs. One of the most investigated MOPs is rhombicuboctahedron with a formula [Cu₂(BDC)₂S₂]₁₂ (S = solvent, BDC = 1,3-benzenedicarboxylate) consisting of 12 dicopper paddlewheel SBUs jointed by 24 1,3-BDC

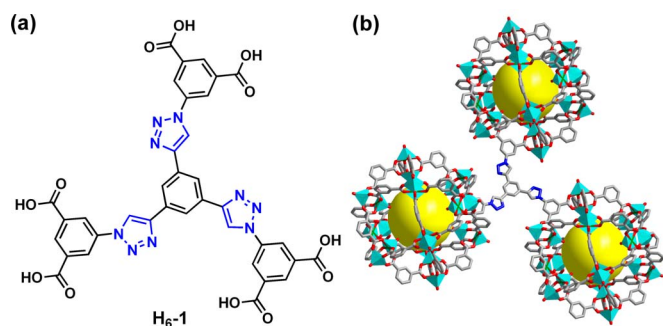


Figure 1 | (a) Chemical structure of ligand **H₆-1** and (b) crystal structure of (3,24)-connected *rth*-type framework of **NTU-105**. In the crystal structure, carbon atoms are colored in gray, nitrogen atoms are colored in blue, oxygen atoms are colored in red, copper atoms are colored in green, and hydrogen atoms and solvent molecules were omitted for sake of clarity.

linkers^{25–28}. The 24 vertices from the 5-position of each BDC linker could be decorated to give rise to discrete polyhedra, chains, or networks^{29–33}. Of particular interest among the networks derived from rhombicuboctahedron is (3,24)-connected *rth*-topology, where triangular metal clusters or triangular organic moieties are employed to rigidly cross-link three BDC ligands^{24,34–41}. Such isoreticular MOFs with *rth*-topology possess a series of specific advantages, including extra-high surface area and pore volume with robust networks, the absence of framework interpenetration, and high concentration of open-metal sites upon the removal of axially coordinated solvent molecules. These salient features enable them to serve as promising porous materials for gas storage and separation.

The modular nature of the *rth*-topology provides an ideal platform for the development of novel MOF materials with the same topology through rational combinations of such well-defined SBBs with suitable ligands that consist of three coplanar BDC units having an overall *C*₃-symmetry (Figure S1 in the Supplementary Information (SI))^{34–41}. In order to introduce nitrogen-rich units into highly porous MOFs by adopting the SBB strategy for enhancing the gas uptake capacity, a *C*₃-symmetric triazole-containing dendritic hexacarboxylate linker, i.e., 5,5',5''-(4,4',4''-(benzene-1,3,5-triyl) tris(1*H*-1,2,3-triazole-4,1-diyl))trisisophthalic acid (**H₆-1** in Figure 1), was designed and subsequently, a nitrogen-rich *rth*-MOF (**NTU-105**) incorporated with coordination-free triazole units was successfully synthesized. Herein, we present the successful fabrication of the nitrogen-rich *rth*-MOF, **NTU-105**, which shows high stability and

large porosity and, as expected, exhibits significantly enhanced gas uptake capacity towards CO₂ and H₂ in comparison with its isoreticular analogues. The roles of the nitrogen-rich triazole units in the framework of **NTU-105** for enhanced gas uptake capacity were demonstrated by both experimental measurements and theoretical molecular simulations.

Results

Synthesis of NTU-105. Based on rational design, the dendritic hexacarboxylate ligand **H₆-1** was conveniently synthesized in high yield by the reaction between 1,3,5-triethynylbenzene and pre-synthesized di-*tert*-butyl 5-azidoisophthalate through click chemistry, i.e. copper(I)-catalyzed azide-alkyne cycloaddition⁴², followed by deprotection in trifluoroacetic acid (see details in the SI). Here, *tert*-butyl group in di-*tert*-butyl 5-azidoisophthalate was introduced in order to increase the solubility of the precursor compound. For the construction of a MOF without the competitive coordination between these Lewis basic nitrogen sites and metal ions, drops of HNO₃ were added in the reaction system. After solvothermal reaction of ligand **H₆-1** with Cu(NO₃)₂·3H₂O in *N,N*-dimethylformamide (DMF) at 75 °C for 3 days, blue crystals of **NTU-105** were obtained and characterized (Figures S2 and S3 in the SI).

Structural characterization. Single-crystal X-ray diffraction investigations revealed that **NTU-105** was crystallized in tetragonal system with space group *I4/m*, having the framework formula of [Cu₃(1)(H₂O)₃]_n (Table S1 in the SI). As expected, in the crystal structure, each organic linker 1 connects with three 24-connected SBBs while leaving the triazole moieties free of coordination (Figures 1 and S4–S6 in the SI). Each SBB consists of 12 dicopper paddlewheels joined by 24 1,3-BDC linkers^{34–41}. **NTU-105** shares the same (3,24)-connected network as prototypical *rth*-type MOF and isoreticular NOTT-112 and PCN-6X^{34–37}. In addition, there are three types of cages within **NTU-105**, namely, cuboctahedron (cub-*O_h*), truncated tetrahedron (T-*T_d*), and truncated octahedron (T-*O_h*), with inner sphere diameters of about 12, 15, and 20 Å, respectively (Figures 2 and S5 in the SI). Powder X-ray diffraction (PXRD) measurements confirmed high phase purity and crystallinity of the bulk sample of as-synthesized **NTU-105** (Figure S7 in the SI).

Chemical and thermal stability. The as-synthesized crystals of **NTU-105** are insoluble in common organic solvents including dichloromethane, chloroform, acetone, acetonitrile, toluene, DMF, and dimethyl sulfoxide (DMSO). The solvent molecules in **NTU-105** can be easily exchanged by some organic solvents such as

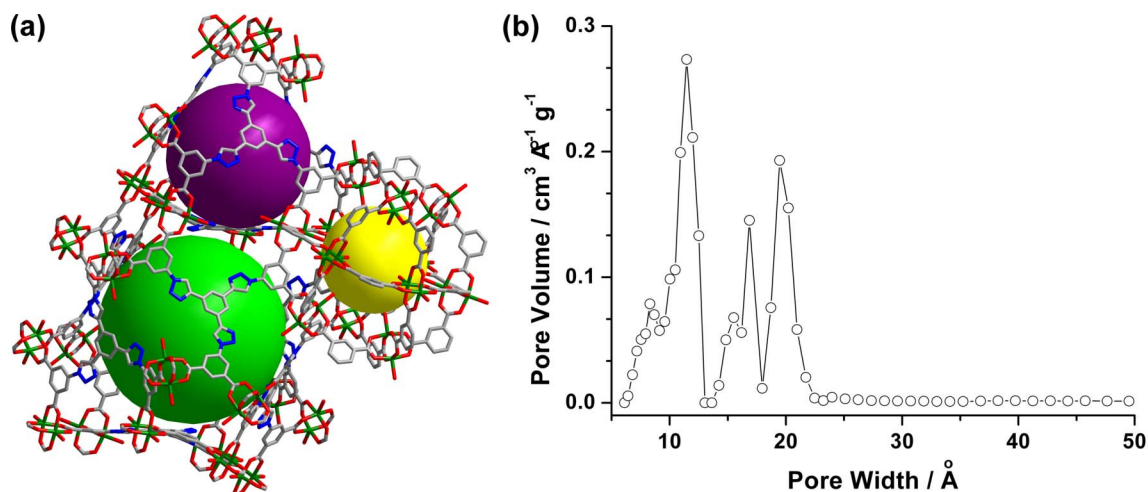


Figure 2 | (a) Three different cages, indicated as yellow, purple, and green balls, in the crystal structure of **NTU-105**, and (b) pore-size distribution plot calculated from experimental Ar adsorption isotherm using the nonlocal density functional theory (NLDFT).



dichloromethane. Thermogravimetric analysis (TGA) was used to verify the thermal stability of NTU-105 (Figure S8 in the SI). The as-synthesized crystalline samples lost the solvent molecules below 260 °C in N₂ flow. When using the desolvated sample of NTU-105 instead of the as-synthesized NTU-105, only a plateau was observed from 80 to 260 °C in the TGA profile, indicating there was nearly no weight loss. Both samples started to decompose rapidly to produce CuO above 260 °C. The desolvated sample of NTU-105 is stable in dry environment, and the structural integrity of the framework is retained as verified by PXRD (Figure S7 in the SI).

Porosity. After removing the guest solvents and coordinated water molecules, the total solvent-accessible volume of desolvated NTU-105 is estimated to be 75.7% using the PLATON/VOID routine⁴³, and the calculated density of the desolvated framework is 0.598 g cm⁻³. To confirm the porosity, NTU-105 was activated sequentially under vacuum at 60 and 120 °C, after exchanging the solvent with dichloromethane. A color change from green-blue to deep purple-blue was observed, which is a typical phenomenon for dicopper-based paddlewheel frameworks where the open Cu^{II} sites were generated during the activation process. The PXRD pattern of the desolvated sample matches very well with the calculated pattern based on the crystal data (Figure S7 in the SI), indicating the retention of the framework after the activation. Then, nitrogen sorption at 77 K was carried out for the activated NTU-105, exhibiting a reversible pseudo-type I sorption isotherm with a quickly increased step prior to the plateau (Figure S9 in the SI)⁴⁴. The observations indicate that NTU-105 possesses both micro- and mesopores^{24,34,35}. The overall nitrogen uptake is 861 cm³ g⁻¹ at 1 atm. The Brunauer-Emmett-Teller (BET) surface area was calculated to be 3543 m² g⁻¹ (Figure S9 in the SI). The total pore volume calculated from nitrogen isotherm is 1.33 cm³ g⁻¹. The pore size distribution, calculated from the analysis of argon sorption isotherm at 87 K based on the non-local density functional theory, reveals peaks at 11, 17, and 19 Å respectively (Figures 2 and S10 in the SI), consistent well with the dimensions of the cages determined in the crystal structure of NTU-105, indicating that the desolvated NTU-105 presents high porosity.

Experimental and theoretical CO₂ uptake capability. The high porosity and stability together with the coordination-free triazole moieties and open metal sites are favorable to the interactions between gas molecules and the framework of NTU-105, which inspired us to investigate its gas uptake capacity and selectivity towards CO₂. As shown in Figure 3, CO₂ sorption isotherms reveal an uptake capability of NTU-105 as high as 187 cm³ g⁻¹ (36.7 wt%) at 1 atm and 273 K, which makes NTU-105 a top MOF material for

CO₂ uptake reported to date^{17,18}, including its isoreticular MOFs containing acylamide groups, amine units, or triazine moieties (i.e., 42.6% for Cu-TPBTM³⁹ and 44.5% for Cu-TDPAT⁴¹). For comparison, the N₂ uptake of NTU-105 at 273 K and 1 atm was measured to be only 16 cm³ g⁻¹. The high adsorption selectivity of NTU-105 towards CO₂ over N₂ under the same conditions (Figure 3) indicates that NTU-105 is highly applicable in the separation of CO₂ over N₂. Then, the isosteric heat of adsorption (Q_{st}) for CO₂ was calculated based on the adsorption isotherms at different temperatures (273 and 298 K, Figure S11 in the SI) through Clausius-Clapeyron equation¹⁷. It was found that Q_{st} is ~35 kJ mol⁻¹ at low loading range, followed by the convergence into a pseudo-plateau (~24 kJ mol⁻¹) with relatively high uptake, the observations which are indicative of strong CO₂-framework interactions. The Q_{st} value at low loading range is the second highest one among the reported *rth*-MOFs, while Cu-TDPAT presents the highest value (42.2 kJ mol⁻¹) so far⁴¹.

The remarkable CO₂-framework interactions were further supported by molecular simulation studies (Figure 4 and S12–S14 in the SI). In order to estimate the charges of the atoms in NTU-105, density functional theory (DFT) calculation was performed in a fragmental cluster shown in Figure 4, and the Lee-Yang-Parr correlation function was employed with Gaussian 03⁴⁵. To investigate the interactions between the adsorbate and the framework, radial distribution functions $g(r)$ were calculated by:

$$g_{ij}(r) = \frac{N_{ij}(r, r + \Delta r) V}{4\pi r^2 \Delta r N_i N_j}$$

where r is the distance between atoms i and j , $N_{ij}(r, r + \Delta r)$ is the number of atom j around i within a shell from r to $r + \Delta r$, V is the system volume, and N_i and N_j are the numbers of atoms i and j , respectively. Figure 4 and Figure S14 show the radial distribution functions of CO₂ around Cu and N1, N2 and N3 atoms on the triazole ring at 1 kPa, 10 kPa and 100 kPa, respectively. Under the pressure range from low to high values (e.g. from 1–100 kPa), all of the three N atoms from the coordination-free triazole unit show high affinities with CO₂. In particular, the N1 atom that is closer to metal cluster shows the strongest interaction with CO₂ than those of the N2 and N3 atoms. From the simulation studies, not only the open Cu^{II} sites within NTU-105 as in other isoreticular *rth*-MOFs, but also the introduced nitrogen-rich triazole units were identified as the preferential interaction sites for CO₂. Thus, the obtained results clearly demonstrate that the coordination-free nitrogen-rich triazole moieties and open metal sites within the framework serve as strong interaction sites, mainly responsible for the high and selective CO₂ uptake.

H₂ uptake capacity. A further application of NTU-105 for the uptake of clean energy, H₂, was investigated. The desolvated NTU-105 exhibits an exceptionally high H₂ uptake capacity up to 308 cm³ g⁻¹ (2.75 wt%) at 77 K and 1 atm (Figure 3), which is the highest value at low pressures in comparison with other isoreticular *rth*-MOFs (Table S2 in the SI)^{46,47}. The isosteric heat of adsorption (Q_{st}) for H₂ was calculated from the isotherms at 77 and 87 K by using Clausius-Clapeyron equation (Figure S15 in the SI)^{46,47}. The Q_{st} value at low coverage was estimated to be 6.61 kJ mol⁻¹, and it was gradually reduced to 5.07 kJ mol⁻¹ upon increasing the coverage. The present average Q_{st} value is similar to the average isosteric heat (~6.1 kJ mol⁻¹) of H₂ uptake in the case of HKUST-1⁴⁸. In the low-pressure region, the H₂ uptake capacity is mainly controlled by its affinity with the framework. Taking into account of the structural similarity and differences with other *rth*-MOFs, the remarkable H₂ uptake capacity of NTU-105 should be attributed to the synergistic effect of the coordination-free nitrogen-rich triazole units and opening metal sites towards H₂ molecules. In addition, the H₂ uptake isotherms predicted from computational simulations match fairly well with the experimental measurements (Figure S13 in the SI).

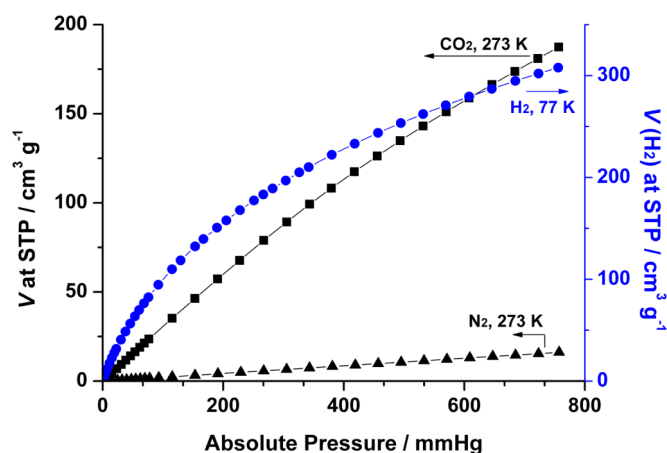


Figure 3 | Gas adsorption isotherms of activated NTU-105 for CO₂ and N₂ measured at 273 K, and H₂ measured at 77 K.

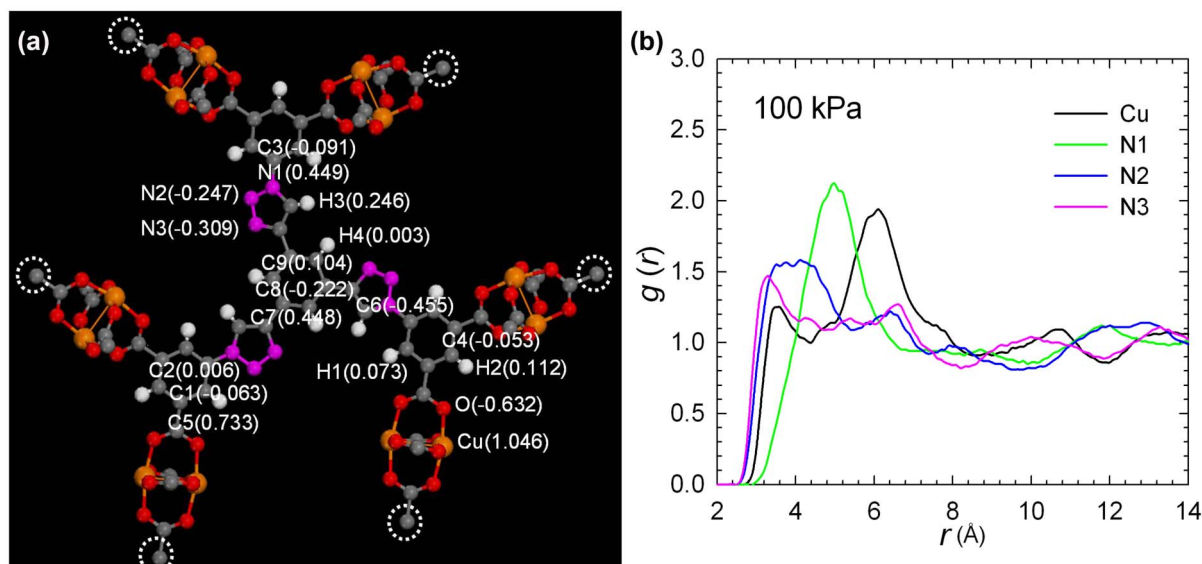


Figure 4 | (a) Atomic charges in a fragmental cluster of NTU-105. The dangling bonds, indicated by white circles, were terminated by hydrogen atoms. Color code: Cu, orange; O, red; N, pink; C, grey; H, white. (b) Radial distribution functions of CO₂ around Cu, N1, N2 and N3 atoms at 100 kPa.

Discussion

Based on the understanding of isorecticular MOFs along with the concept of supermolecular building blocks, a dendritic nitrogen-rich hexacarboxylate ligand has been designed and synthesized by utilizing click chemistry, which has been employed to construct a (3,24)-connected MOF (NTU-105) with the *rth*-type topology. As compared with reported amino-functionalized MOFs in literature^{11–16,39,41}, this is the first time that nitrogen-rich triazole units are successfully introduced onto the struts of an *rth*-type MOF targeted for CO₂ capture and storage. On account of the easy and efficient approach of using click chemistry in the preparation of triazole-containing MOF for selective gas adsorption, one can envisage that more delicate nitrogen-rich MOFs as efficient adsorbents could be developed.

Comparing with some of reported isorecticular MOFs^{34–41}, the present nitrogen-rich NTU-105 possesses the BET surface area of only 3543 m² g^{−1}, but exhibits exceptionally high CO₂ (36.7 wt% at 273 K and 1 atm) and H₂ (2.75 wt% at 77 K and 1 atm) uptake capacities. The simulation studies have confirmed that the coordination-free triazole moieties and the open metal sites within the framework provide strong interactions with the gas molecules, thus leading to significantly enhanced gas uptake capacity and selectivity. Since the gas uptake capacity of porous materials is not always proportional to their surface areas, engineering nitrogen-rich organic units within porous materials to enhance the adsorption affinity towards specific gas molecules, especially CO₂, would be one of the ideal and convenient choices for gas adsorption and selective separation on the way towards a sustainable future.

In summary, we have designed and synthesized a (3,24)-connected nitrogen-rich *rth*-MOF. The nitrogen-rich MOF exhibits high thermal stability and large porosity along with exceptionally high CO₂ and H₂ uptake capacities. Both the experimental measurements and theoretical molecular simulations have indicated that, although the BET surface area of nitrogen-rich MOF is not significantly high as compared with some of its isorecticular MOFs^{34–41}, the incorporation of accessible nitrogen-donor sites into the framework dramatically enhances its gas uptake capacity and selectivity.

Methods

Synthesis of H₆-1. In a degassed THF/H₂O (100 mL/40 mL) solution containing 1,3,5-triethynylbenzene (0.21 g, 1.40 mmol) and di-tert-butyl 5-azidoisophthalate (1.55 g, 4.85 mmol), CuSO₄ (0.11 g, 0.44 mmol) and sodium ascorbate (0.17 g, 0.86 mmol) were added and the mixture solution was stirred at 60 °C under Ar for

3 days. Ester 'Bu₆-1 (1.10 g, 0.99 mmol, yield: 71%) was obtained after purifying the crude product through silica gel flash column chromatography (CH₂Cl₂/EtOAc, 100/1). Then, trifluoroacetic acid (TFA, 10 mL) was added to a CH₂Cl₂ solution (20 mL) of 'Bu₆-1 (1.23 g, 1.11 mmol), and mixture solution was stirred at room temperature over 5 h. The suspension was filtered and washed with CH₂Cl₂, and the obtained solid was dried under vacuum to afford the compound H₆-1 (0.73 g, 0.95 mmol, yield: 86%) as white solid. ¹H NMR (500 MHz, DMSO) δ 9.64 (s, 3H), 8.68 (s, 6H), 8.53 (s, 3H), 8.48 (s, 3H). ¹³C NMR (101 MHz, DMSO) δ 165.6, 147.0, 136.6, 132.8, 130.8, 129.1, 122.9, 121.6, 119.0. ESI-TOF-HRMS: *m/z* calcd for C₃₆H₂₂N₉O₁₂: 772.1388, found: 772.1384 [M+H]⁺.

Synthesis of NTU-105. Compound H₆-1 (21 mg, 0.03 mmol) and Cu(NO₃)₂·3H₂O (22 mg, 0.09 mmol) were dissolved in DMF (12 mL). Then, drops of HNO₃ (1.5 mol L^{−1}, 60 drops) were added into the solution. The mixture solution was placed in a tightly capped 20 mL vial, which was heated in an oven at 75 °C for 3 days. The light blue block crystals of NTU-105 were collected after cooling the sample down to room temperature. These crystals were washed by fresh DMF for 3 times, and dried under vacuum. The obtained crystals were subjected to elemental analysis and TGA analysis in order to estimate the empirical formula as Cu₃(1)(H₂O)₃·11DMF·8H₂O (44.8 mg, yield: 76% based on H₆-1). Elemental analysis calcd (%) for Cu₃C₆₉H₁₂₀N₂₀O₃₄: C 42.19, H 6.16, N 14.26; found: C 42.17, H 6.48, N 14.33. IR (KBr) (cm^{−1}): 1652 (s), 1583 (m), 1428 (m), 1379 (s), 1104 (m), 1063 (m), 777 (m).

- Rosi, N. L. *et al.* Hydrogen storage in microporous metal-organic frameworks. *Science* **300**, 1127–1129 (2003).
- Bloch, E. D. *et al.* Hydrocarbon separations in a metal-organic framework with open iron(II) coordination sites. *Science* **335**, 1606–1610 (2012).
- Li, Q. *et al.* Docking in metal-organic frameworks. *Science* **325**, 855–859 (2009).
- Ma, L., Abney, C. & Lin, W. Enantioselective catalysis with homochiral metal-organic frameworks. *Chem. Soc. Rev.* **38**, 1248–1256 (2009).
- Keskin, S. & Kizilel, S. Biomedical applications of metal-organic frameworks. *Ind. Eng. Chem. Res.* **50**, 1799–1812 (2011).
- Kitagawa, S., Kitaura, R. & Noro, S.-I. Functional porous coordination polymers. *Angew. Chem. Int. Ed.* **43**, 2334–2375 (2004).
- O'Keeffe, M. & Yaghi, O. M. Deconstructing the crystal structures of metal-organic frameworks and related materials into their underlying nets. *Chem. Rev.* **112**, 675–702 (2012).
- Tang, L. *et al.* A zeolite family with chiral and achiral structures built from the same building layer. *Nat. Mater.* **7**, 381–385 (2008).
- Kuchta, B. *et al.* Hypothetical high-surface-area carbons with exceptional hydrogen storage capacities: Open carbon frameworks. *J. Am. Chem. Soc.* **134**, 15130–15137 (2012).
- Vogiatzis, K. D., Mavrandonakis, A., Kloppe, W. & Froudakis, G. E. *Ab initio* study of the interactions between CO₂ and N-containing organic heterocycles. *ChemPhysChem* **10**, 374–383 (2009).
- Vaidhyanathan, R. *et al.* Direct observation and quantification of CO₂ binding within an amine-functionalized nanoporous solid. *Science* **330**, 650–653 (2010).
- Vaidhyanathan, R., Iremonger, S. S., Dawson, K. W. & Shimizu, G. K. H. An amine-functionalized metal organic framework for preferential CO₂ adsorption at low pressures. *Chem. Commun.* 5230–5232 (2009).



13. Couck, S. *et al.* An amine-functionalized MIL-53 metal-organic framework with large separation power for CO₂ and CH₄. *J. Am. Chem. Soc.* **131**, 6326–6327 (2009).
14. Wang, F., Tan, Y.-X., Yang, H., Kang, Y. & Zhang, J. Open diamondoid amino-functionalized MOFs for CO₂ capture. *Chem. Commun.* **48**, 4842–4844 (2012).
15. Du, N. *et al.* Polymer nanosieve membranes for CO₂-capture applications. *Nat. Mater.* **10**, 372–375 (2011).
16. Wang, X.-J. *et al.* Significant gas uptake enhancement by post-exchange of zinc(II) with copper(II) within a metal-organic framework. *Chem. Commun.* **48**, 10286–10288 (2012).
17. Sumida, K. *et al.* Carbon dioxide capture in metal-organic frameworks. *Chem. Rev.* **112**, 724–781 (2012).
18. Li, J.-R. *et al.* Carbon dioxide capture-related gas adsorption and separation in metal-organic frameworks. *Coord. Chem. Rev.* **255**, 1791–1823 (2011).
19. Zhang, J.-P., Zhang, Y.-B., Lin, J.-B. & Chen, X.-M. Metal azolate frameworks: From crystal engineering to functional materials. *Chem. Rev.* **112**, 1001–1033 (2012).
20. Aromí, G., Barrios, L. A., Roubeau, O. & Gamez, P. Triazoles and tetrazoles: Prime ligands to generate remarkable coordination materials. *Coord. Chem. Rev.* **255**, 485–546 (2011).
21. Ockwig, N. W., Delgado-Friedrichs, O., O’Keeffe, M. & Yaghi, O. M. Reticular chemistry: Occurrence and taxonomy of nets and grammar for the design of frameworks. *Acc. Chem. Res.* **38**, 176–182 (2005).
22. Yaghi, O. M. *et al.* Reticular synthesis and the design of new materials. *Nature* **423**, 705–714 (2003).
23. Perry IV, J. J., Perman, J. A. & Zaworotko, M. J. Design and synthesis of metal-organic frameworks using metal-organic polyhedra as supermolecular building blocks. *Chem. Soc. Rev.* **38**, 1400–1417 (2009).
24. Cairns, A. J. *et al.* Supermolecular building blocks (SBBs) and crystal design: 12-Connected open frameworks based on a molecular cubohemioctahedron. *J. Am. Chem. Soc.* **130**, 1560–1561 (2008).
25. Nouar, F. *et al.* Supermolecular building blocks (SBBs) for the design and synthesis of highly porous metal-organic frameworks. *J. Am. Chem. Soc.* **130**, 1833–1835 (2008).
26. Eddaoudi, M. *et al.* Porous metal-organic polyhedra: 25 Å Cuboctahedron constructed from 12 Cu₂(CO₂)₄ paddle-wheel building blocks. *J. Am. Chem. Soc.* **123**, 4368–4369 (2001).
27. Moulton, B., Lu, J., Mondal, A. & Zaworotko, M. J. Nanoballs: Nanoscale faceted polyhedra with large windows and cavities. *Chem. Commun.* 863–864 (2001).
28. Tranchemontagne, D. J., Ni, Z., O’Keeffe, M. & Yaghi, O. M. Reticular chemistry of metal-organic polyhedra. *Angew. Chem. Int. Ed.* **47**, 5136–5147 (2008).
29. McManus, G. J., Wang, Z. & Zaworotko, M. J. Suprasupermolecular chemistry: Infinite networks from nanoscale metal-organic building blocks. *Cryst. Growth Des.* **4**, 11–13 (2004).
30. Furukawa, H., Kim, J., Plass, K. E. & Yaghi, O. M. Crystal structure, dissolution, and deposition of a 5 nm functionalized metal-organic great rhombicuboctahedron. *J. Am. Chem. Soc.* **128**, 8398–8399 (2006).
31. Perry IV, J. J., Kravtsov, V. C., McManus, G. J. & Zaworotko, M. J. Bottom up synthesis that does not start at the bottom: Quadruple covalent cross-linking of nanoscale faceted polyhedra. *J. Am. Chem. Soc.* **129**, 10076–10077 (2007).
32. Wang, X.-S. *et al.* Enhancing H₂ uptake by “close-packing” alignment of open copper sites in metal-organic frameworks. *Angew. Chem. Int. Ed.* **47**, 7263–7266 (2008).
33. Li, J.-R. & Zhou, H.-C. Bridging-ligand-substitution strategy for the preparation of metal-organic polyhedra. *Nat. Chem.* **2**, 893–898 (2010).
34. Yan, Y. *et al.* Exceptionally high H₂ storage by a metal-organic polyhedral framework. *Chem. Commun.* 1025–1027 (2009).
35. Zhao, D., Yuan, D., Sun, D. & Zhou, H.-C. Stabilization of metal-organic frameworks with high surface areas by the incorporation of mesocavities with microwindows. *J. Am. Chem. Soc.* **131**, 9186–9188 (2009).
36. Yan, Y. *et al.* Metal-organic polyhedral frameworks: High H₂ adsorption capacities and neutron powder diffraction studies. *J. Am. Chem. Soc.* **132**, 4092–4094 (2010).
37. Yuan, D., Zhao, D., Sun, D. & Zhou, H.-C. An isoreticular series of metal-organic frameworks with dendritic hexacarboxylate ligands and exceptionally high gas-uptake capacity. *Angew. Chem. Int. Ed.* **49**, 5357–5361 (2010).
38. Farha, O. K. *et al.* De novo synthesis of a metal-organic framework material featuring ultrahigh surface area and gas storage capacities. *Nature Chem.* **2**, 944–948 (2010).
39. Zheng, B., Bai, J., Duan, J., Wojtas, L. & Zaworotko, M. J. Enhanced CO₂ binding affinity of a high-uptake *rht*-type metal-organic framework decorated with acylamide groups. *J. Am. Chem. Soc.* **133**, 748–751 (2011).
40. Farha, O. K. *et al.* Designing higher surface area metal-organic frameworks: Are triple bonds better than phenyls? *J. Am. Chem. Soc.* **134**, 9860–9863 (2012).
41. Li, B. *et al.* Enhanced binding affinity, remarkable selectivity, and high capacity of CO₂ by dual functionalization of a *rht*-type metal-organic framework. *Angew. Chem. Int. Ed.* **51**, 1412–1415 (2012).
42. Rostovtsev, V. V., Green, L. G., Fokin, V. V. & Sharpless, K. B. A stepwise Huisgen cycloaddition process: Copper(I)-catalyzed regioselective “ligation” of azides and terminal alkynes. *Angew. Chem. Int. Ed.* **41**, 2596–2599 (2002).
43. Spek, A. Structure validation in chemical crystallography. *Acta Crystallogr. Sect. D* **65**, 148 (2009).
44. Sing, K. S. W. *et al.* Reporting physisorption data for gas/solid systems with special reference to the determination of surface area and porosity. *Pure Appl. Chem.* **57**, 603–619 (1985).
45. Frisch, M. J. *et al.* *Gaussian 03*, Revision D.01 ed.; Gaussian, Inc., Wallingford CT, 2004.
46. Suh, M. P., Park, H. J., Prasad, T. K. & Lim, D.-W. Hydrogen storage in metal-organic frameworks. *Chem. Rev.* **112**, 782–835 (2012).
47. Murray, L. J., Dincă, M. & Long, J. R. Hydrogen storage in metal-organic frameworks. *Chem. Soc. Rev.* **38**, 1294–1314 (2009).
48. Krawiec, P. *et al.* Improved hydrogen storage in the metal-organic framework Cu₃(BTC)₂. *Adv. Eng. Mater.* **8**, 193–196 (2006).

Acknowledgments

We thank the financial support of the Singapore National Research Foundation Fellowship (NRF2009NRF-RF001-015), Singapore National Research Foundation CREATE program – Singapore Peking University Research Centre for a Sustainable Low-Carbon Future, and Nanyang Technological University.

Author contributions

X.J.W. and P.Z.L. designed and carried out the experiments. Y.C. and J.J. carried out the molecular simulations. R.G. and Y.L. performed the major part of single crystal X-ray diffraction analysis. Q.Z., H.Z. and X.X. Chan joined in the experiments and discussions. X.J.W., P.Z.L. and Y.Z. discussed and analyzed the data, interpreted the results and jointly wrote the paper.

Additional information

Supplementary information accompanies this paper at <http://www.nature.com/scientificreports>

Competing financial interests: The authors declare no competing financial interests.

License: This work is licensed under a Creative Commons

Attribution-NonCommercial-No Derivs 3.0 Unported License. To view a copy of this license, visit <http://creativecommons.org/licenses/by-nc-nd/3.0/>

How to cite this article: Wang, X. *et al.* A Rationally Designed Nitrogen-Rich Metal-Organic Framework and Its Exceptionally High CO₂ and H₂ Uptake Capability. *Sci. Rep.* **3**, 1149; DOI:10.1038/srep01149 (2013).